Xsim: A Unified Compact Model for Bulk/SOI/DG/GAA MOSFETs

Xing Zhou

School of Electrical and Electronic Engineering
Nanyang Technological University
Nanyang Avenue, Singapore 639798, exzhou@ntu.edu.sg

ABSTRACT

This paper presents a unified compact model (Xsim) for bulk/SOI MOSFETs, double-gate (DG) FinFETs, and gate-all-around (GAA) silicon-nanowires (SiNWs) that has been under development over the past 13 years. One key feature of the model is complete scalability with body doping and thickness, encompassing conventional bulk and partially-depleted (PD) SOI and emerging fully-depleted (FD) ultrathin body (UTB) SOI and DG/GAA FinFETs/SiNWs. The single core model is achieved with the unified regional modeling (URM) approach for the surface potential in all regions of operation, with body doping ranging from very high to low and undoped (pure Si). Some unique features that do not appear in other contemporary compact models include: ground-reference for floating-body (FB) SOI and DG/GAA devices with complete symmetry and physical modeling of asymmetric source/drain (S/D) without swapping S/D terminal polarities for V_{ds} changing signs; gate-bias dependent S/D series resistance in all regions; velocity-overshoot modeling with the electron-temperature gradient term added to the conventional drift-diffusion formalism; seamless transition from depletion to volume/strong inversion for all ranges of body doping and thickness. Other major modeled effects include: vertical/lateral nonuniform doping; longitudinal/transverse-field mobility; quasi-2D solution for drain-induced barrier lowering (DIBL) and velocity saturation/overshoot; poly-gate accumulation/ depletion/inversion effect (PAE/PDE/PIE); quantum-mechanical effect (QME); short-channel intrinsic/ extrinsic charge model with URM of surface potential. The Xsim model has also been extended to strained-Si/SiGe channel and dopant-segregated Schottky-barrier (SB) MOSFETs, as well as physical modeling of interface traps for reliability and statistical-CM for variation and mismatch studies. The model has a small set of parameters (< 40) that requires minimum data and one or two-iteration parameter extraction. The ultimate goal of the Xsim model is for unification of MOSFET compact models with various gate, body, as well as source/drain structures and dimensions in one unified core framework for simulating and designing integrated circuits in future generation technologies.

Keywords: Compact model (CM), double-gate (DG), gate-all-around (GAA), MOSFET, silicon nanowire (SiNW), ultrathin body (UTB) SOI, unified regional modeling (URM), Xsim.

1 INTRODUCTION

The mainstream CMOS technology has evolved over half a century, from the early "long-channel" metal-oxide-semiconductor (MOS) bulk devices through continued scaling with poly-Si gate to today's nanoscale devices with high-K/metal-gate, including various alternative structures such as ultrathin-body (UTB) SOI as well as double-gate (DG) FinFETs and gate-all-around (GAA) silicon-nanowire (SiNW) devices. The compact models (CMs) describing terminal characteristics of various devices also evolve over the years with different formulations [1], such as threshold-voltage (V_t)-based, inversion-charge (Q_i)-based, and surface-potential (ϕ_s)-based models. It has been recognized the importance of building in the correct physics while making approximations in formulating *scalable* CMs with minimum number of fitting parameters. When a physically scalable model is not available, empirical fitting will have to be adopted in order to solve real problems in practice, such as "binning" model in geometry scaling, "age-binning" with a fresh-device model for reliability, or fitting a Si-MOS model to a carbon-nanotube (CNT) or organic-FET device.

In this paper, we discuss the need for a unified CM for various types of MOS devices and the underlying requirements for seamless transitions among different device structures and operations. This is demonstrated with the unified regional modeling (URM) approach as adopted in the development of the Xsim model. Detailed Xsim formulations have been reviewed in a recent article [2] and the references therein. Major benchmark tests of the Xsim model has been presented in [3].

2 THE XSIM MODEL

All CM formulations start with solving Poisson's equation with the carrier concentrations approximated by the Boltzmann's relation under nonequilibrium conditions

$$n = n_i e^{(\phi-\phi_{Fn})/v_{th}} = n_i e^{(\phi-\phi_F-V_c)/v_{th}} \quad \text{(1a)}$$

$$p = n_i e^{-(\phi-\phi_{Fp})/v_{th}} = n_i e^{-(\phi-\phi_F-V_r)/v_{th}} \quad \text{(1b)}$$

where the electron imref ($\phi_{Fn} = \phi_F + V_c$) varies from source ($\phi_F + V_s$) to drain ($\phi_F + V_d$) when $V_{ds} \neq 0$ while the hole imref ($\phi_{Fp} = \phi_F + V_r$) is assumed constant (for nMOS), in which V_r is taken as the potential reference, i.e., $V_r = 0$ at $V_{gf} \equiv V_{gr} - V_{FB} = 0$ (flatband) and $V_{ds} = 0$ (equilibrium).

With charge neutrality (in the neutral body, or at least at flatband condition),

$$n_0 \equiv n(\phi = V_r) = n_i e^{-(\phi_F + V_{cr})/v_{th}} \tag{2a}$$

$$p_0 \equiv p(\phi = V_r) = n_i e^{\phi_F / v_{th}} \tag{2b}$$

$$N_A - N_D = p_0 - n_0 \tag{2}$$

the Poisson–Boltzmann (PB) equation is given by

$$\begin{aligned} \frac{d^2\phi}{dx^2} &= -\frac{\rho}{\varepsilon_{Si}} = -\frac{q(p - n + N_D - N_A)}{\varepsilon_{Si}} \\ &= \frac{qp_0}{\varepsilon_{Si}}\left[e^{(\phi - 2\phi_F - V_c)/v_{th}} - e^{-(\phi - V_r)/v_{th}} + 1 - e^{-(2\phi_F + V_{cr})/v_{th}}\right] \end{aligned} \tag{3}$$

The first integral of the PB equation (2) from surface ($x = 0$) to the zero-field (ZF) location ($x = X_o$), with Gauss' law applied at the surface, is given by

$$V_{gf} - \phi_s = \mathrm{sgn}(\phi_s - \phi_o)\, \Upsilon \sqrt{f_\phi(\phi_s, \phi_o, V_c, V_r)} \tag{4}$$

$$\begin{aligned} f_\phi = {} & \underbrace{e^{-(2\phi_F + V_{cr})/v_{th}}\left[v_{th} e^{-V_r/v_{th}}\left(e^{\phi_s/v_{th}} - e^{\phi_o/v_{th}}\right)}_{(n)} - \underbrace{(\phi_s - \phi_o)\Big]}_{(n_0)} \\ & + \underbrace{v_{th} e^{V_r/v_{th}}\left(e^{-\phi_s/v_{th}} - e^{-\phi_o/v_{th}}\right)}_{(p)} + \underbrace{(\phi_s - \phi_o)}_{(p_0)} \end{aligned} \tag{4a}$$

$$\Upsilon = \sqrt{2q\varepsilon_{Si} p_0} \big/ C_{ox} \tag{4b}$$

in which the equilibrium (majority) hole concentration is given by (2b)

$$p_0 = n_i e^{\phi_F/v_{th}} = n_i \exp\left[\sinh^{-1}\left(\frac{N_A - N_D}{2n_i}\right)\right] \tag{5a}$$

with the Fermi potential given by the well-known Kingston equation [4]

$$\phi_F = v_{th} \sinh^{-1}\left(\frac{N_A - N_D}{2n_i}\right) \tag{5b}$$

which approaches the conventional formula

$$\phi_F \approx v_{th} \ln\left(\frac{N_A}{n_i}\right) \tag{5c}$$

when the body doping is very high ($N_A >> n_i$, $p_0 \approx N_A$).

The ZF location can be determined from the "depletion width" based on full-depletion (FD) approximation

$$\begin{aligned} X_d &= \sqrt{\frac{2\varepsilon_{Si}(\phi_s - \phi_o)}{qp_0}} = \sqrt{\frac{2\varepsilon_{Si}}{qp_0}}\left(-\frac{\Upsilon}{2} + \sqrt{\frac{\Upsilon^2}{4} + V_{gf} - \phi_o}\right) \\ &\leq \sqrt{\frac{2\varepsilon_{Si}(2\phi_F + V_{cr})}{qp_0}} = X_{dm} \end{aligned} \tag{6}$$

In the above formulations, the conceptual region of the MOSFET is from source to drain ($0 \leq y \leq L$), excluding the 2D potential profiles at the source/drain (S/D) pn-junctions; and from surface to the ZF location ($0 \leq x \leq X_o$), excluding carrier generation/recombination beyond the FD region; thus, n_0 in (2a) is strictly x independent and includes the y-dependent $V_{cr}(y)$. This is consistent with the solution (4), which requires x-independent V_{cr}, and it is also the physical picture for floating-body (FB) SOI and DG/GAA FinFET/ SiNW devices. For models that assume no V_{cr} dependence in the "remote" minority carriers (n_0), some form of "mathematical conditioning" would be required to avoid imaginary iterative ϕ_s solutions near flatband.

For a generic double-gate (DG) MOSFET, the induced charge in the body may be controlled by both gates, and the solution to the PB equation subject to two boundary conditions requires integrating (3) twice. However, if the doping term is not ignored, it cannot be done analytically. On the other hand, if the doping term is ignored, the PB equation can be integrated twice, but its solution cannot be extended to devices with body doping.

The rationale behind the URM approach is to solve asymptotic regional solutions physically and combine them with smoothing/transition functions seamlessly. Instead of solving the coupled equation with two boundary conditions in the generic DG device, we solve two separate solutions due to each gate including the doping term, and coupling them based on the "FD condition" when the sum of the two individual "depletion widths" by (6) reaches the body thickness (T_{Si}). Since the second "boundary" is taken at the ZF location at which the potential is ϕ_o and field is $E_o = 0$, it is simply replacing the "bulk" solution by subscript '1' for gate-1 and '2' for gate-2. This generic picture includes partially-depleted (PD) and FD SOI as well as symmetric (s-DG), common-asymmetric (ca-DG), and independent-asymmetric (ia-DG) FinFETs and GAA SiNWs. A schematic cross-section of a generic DG nMOSFET is shown in Fig. 1.

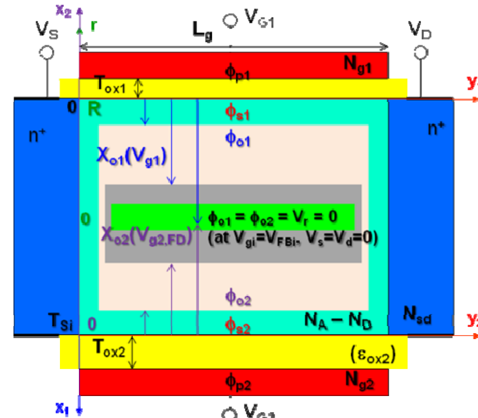

Figure 1: A generic DG nMOSFET in which important physical parameters associated with gate-1 and gate-2 are labeled, respectively, including PD/FD-SOI and s-DG/ca-DG/ia-DG structures. GAA has the similar cross-section as s-DG in cylindrical coordinate. The ZF location X_{oi} ("depletion width" due to gate-i alone, $i = 1, 2$) together with the FD condition links the two gates.

If $T_{Si} < X_d$, "full depletion" occurs when $X_d(V_{g,FD}) = T_{Si}$ based on (6)

$$T_{Si} = X_d\left(V_{g,FD}\right) = \sqrt{\frac{2\varepsilon_{Si}}{qp_0}}\left(-\frac{\Upsilon}{2}+\sqrt{\frac{\Upsilon^2}{4}+V_{gf,FD}-\phi_o}\right) \quad (7a)$$

where $V_{g,FD}$ is the *FD voltage* and $V_{gf,FD} \equiv V_{g,FD} - V_{FB}$. The corresponding *FD potential* is given by

$$\phi_{FD} = \phi_s - \phi_o = \frac{qp_0 X_d^2\left(V_{g,FD}\right)}{2\varepsilon_{Si}} = \left(-\frac{\Upsilon}{2}+\sqrt{\frac{\Upsilon^2}{4}+V_{gf,FD}-\phi_o}\right)^2 \quad (7b)$$

When $V_g < V_{g,FD}$, the body is PD and $\phi_o = V_r = 0$ is the reference potential. Beyond the FD voltage ($V_g > V_{g,FD}$) if strong inversion has not been reached, "volume inversion" will occur, in which the surface potential ϕ_s will follow V_g as in (4) ignoring the p, n, and n_0 terms with a fixed ϕ_{FD} given by (7b). And the *ZF potential* ϕ_o needs to be modeled and included in the ϕ_s solution.

Asymptotic *piecewise regional* solutions to (4) exist, if only the p, p_0, and n terms are considered in accumulation, depletion, volume inversion, and strong inversion, respectively, given by

$$\begin{cases} \phi_{cc} = V_{gf} + 2v_{th}\mathcal{L}\left\{\frac{\Upsilon}{2\sqrt{v_{th}}}e^{-(V_{gf}-V_r)/2v_{th}}\right\} & (V_{gr} < V_{FB}) \\ \phi_{dd} = \phi_o + \left(-\frac{\Upsilon}{2}+\sqrt{\frac{\Upsilon^2}{4}+(V_{gf}-\phi_o)}\right)^2 & (V_{FB} < V_{gr} < V_{g,FD}) \\ \phi_{dv} = V_{gf} - \Upsilon\sqrt{\phi_{FD}} & (V_{g,FD} < V_{gr} < V_t) \\ \phi_{ss} = V_{gf} - 2v_{th}\mathcal{L}\left\{\frac{\Upsilon}{2\sqrt{v_{th}}}e^{(V_{gf}-2\phi_F-V_c)/2v_{th}}\right\} & (V_{gr} > V_t) \end{cases} \quad (8)$$

where $\mathcal{L}\{W\}$ is the *Lambert W* function.

With the following complementary smoothing functions

$$\vartheta_f\{x;\sigma\} = 0.5\left(x+\sqrt{x^2+4\sigma}\right) \quad (9a)$$

$$\vartheta_r\{x;\sigma\} = 0.5\left(x-\sqrt{x^2+4\sigma}\right) \quad (9b)$$

and the following transition function

$$\vartheta_{eff}\{x,x_{sat};\delta\} = x_{sat} - 0.5\left[x_{sat}-x-\delta+\sqrt{(x_{sat}-x-\delta)^2+4\delta x_{sat}}\right] \quad (9c)$$

the single-piece *unified regional* solutions are given by

$$\phi_s = \begin{cases} \phi_{acc} = \vartheta_r\left(V_{gf};\sigma_a\right) + 2v_{th}\mathcal{L}\left\{\frac{\Upsilon}{2\sqrt{v_{th}}}e^{-(V_{gf}-V_r)/2v_{th}}\right\} \\ \phi_{sub} = \phi_o + \left(-\frac{\Upsilon}{2}+\sqrt{\frac{\Upsilon^2}{4}+\vartheta_f\left(V_{gf}-\phi_o;\sigma_f\right)}\right)^2 \\ \phi_{dep} = \vartheta_{eff}\left(\phi_{sub},\phi_{FD};\delta_d\right) \\ \phi_{dv} = V_{gf} - \Upsilon\sqrt{\phi_{FD}} \\ \phi_{str} = \vartheta_f\left(V_{gf};\sigma_s\right) - 2v_{th}\mathcal{L}\left\{\frac{\Upsilon}{2\sqrt{v_{th}}}e^{(V_{gf}-2\phi_F-V_c)/2v_{th}}\right\} \\ \phi_{ds} = \vartheta_{eff}\left(\phi_{dv},\phi_{str};\delta_\phi\right) \\ \phi_{seff} = \phi_{acc} + \phi_{ds} \end{cases} \quad (10)$$

This model covers all types of bulk/SOI/DG/GAA MOSFETs with complete doping scaling. The unique URM behaviors and the corresponding derivatives are shown in Fig. 2 for a heavily-doped s-DG FinFET and compared with the corresponding numerical device data. The physical parameters V_{FB}, V_{FD}, and V_t will scale with device structural and doping parameters, while transitions across various regions are tuned *seamlessly* by the respective smoothing parameters, which do not require any data for fitting and are fixed once tuned. In Fig. 2(a), the FD voltage is determined from

$$X_{o1}\left(V_{g1,FD}\right) + X_{o2}\left(V_{g2,FD}\right) = T_{Si} \quad (11)$$

where $V_{g1} = V_{g1} = V_g$ for s-DG, and the correct "slope" in depletion and volume-inversion regions [Fig. 2(b)] are physically captured by the regional solutions.

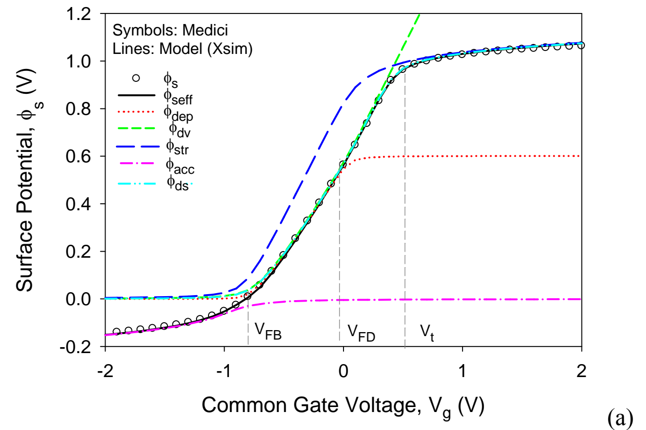

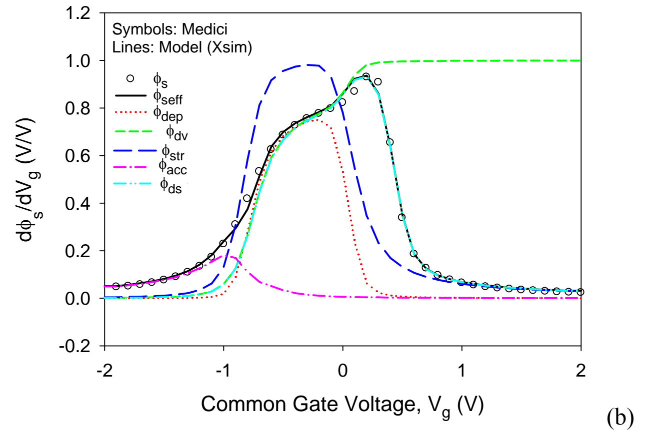

Figure 2: (*a*) Unified (smooth) regional surface-potential solutions in strong invertion (ϕ_{str}), accumulation (ϕ_{acc}), depletion (ϕ_{dep}), depletion- to-volume inversion (ϕ_{dv}), depletion-to-strong inversion (ϕ_{ds}), and single-piece solution (ϕ_{seff}), and (*b*) the corresponding derivatives, compared with Medici data (*circle*) for the s-DG FinFET with T_{ox} = 3 nm, T_{Si} = 50 nm, and a heavily-doped body $N_A = 10^{18}$ cm^{-3}.

2.1 Body-Doping Scaling

For a model with complete body doping scaling, from very high to low (unintentionally doped) and undoped (pure

Si), it is essential to use the Kingston equation for the Fermi potential (5b) and p_0 in the body factor (4b). If N_A is used in (4b), it would give wrong results when N_A approaches n_i. Even for practical cases in which unintentional doping (e.g., $N_A = 10^{14}$ cm^{-3}) is always present, it would approach "intrinsic" semiconductor at high temperatures; thus, (5c) and N_A in (4b) would still give wrong solutions.

If a model formulation starts with undoped body (i.e., zero doping), there will be only volume inversion (no depletion) in the subthreshold region. For practical devices with unintentional doping, even if its effect in shifting the flatband voltage can be easily modeled, the correct physics in the ϕ_s "slope" (*near* unity, by ϕ_{dd}) is different from volume inversion (*exact* unity, by ϕ_{dv}), if the body is extremely thick. Figure 3(a) shows the URM ϕ_s solutions with varying N_A in a thin-body s-DG FinFET, in which volume inversion (unity slope) is observed. If the body were thick, one would expect similar behaviors at low doping but different physics (near-unity slope).

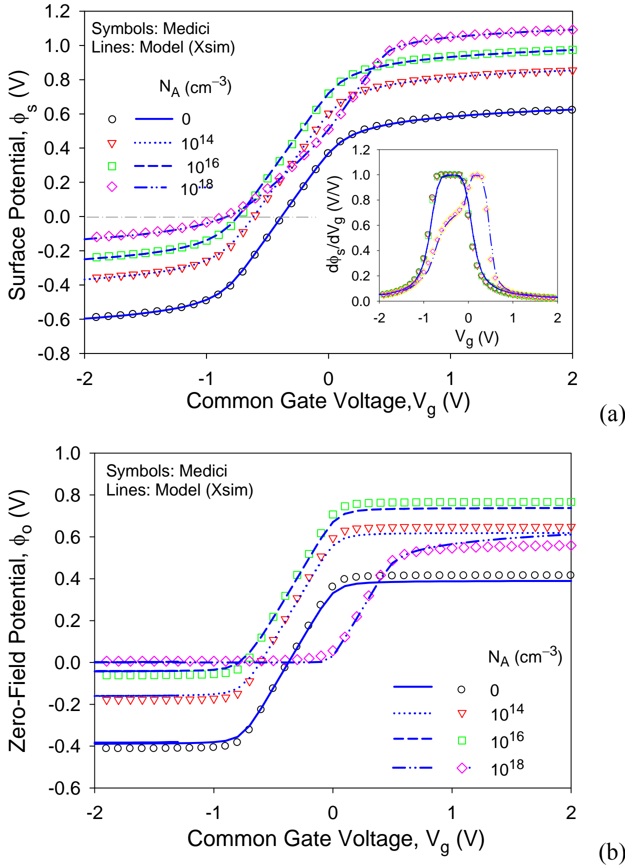

Figure 3: Unified regional (*a*) ϕ_s and (*b*) ϕ_o solutions in all regions at four different body doping as indicated, compared with Medici data (*circle*) for the s-DG FinFET with T_{ox} = 3 nm and T_{Si} = 50 nm. The corresponding derivatives are shown in the inset of (*a*).

For undoped body, ϕ_o needs to be used in calculating the charge and current, and it can be solved since the second integral of the PB equation is available [5]. For highly-doped body, however, the PB equation cannot be integrated twice, and most models assume a constant difference between ϕ_s and ϕ_o as in (7b) with a maximum depletion width by (6). Consistent with the URM approach, unified regional ZF ϕ_o solutions are obtained by considering only the n term in the second integral of the PB equation, given by [5], [2]

$$\phi_{o,ds} = v_{th} \ln\left(\frac{B_{ds}}{A_{ss}}\right) - 2v_{th} \ln\left(\cos\left(\arccos\left(\sqrt{\frac{B_{ds}}{A_{ss}}} e^{-(\phi_{ds}-\phi_{FD})/v_{th}} \right) + \frac{\sqrt{B_{ds}}}{2v_{th}} X_o \right) \right), \quad (12)$$

$$A_{ss} = \left(2qp_0 v_{th} e^{-(2\phi_F + V_{cr})/v_{th}}\right) \big/ \varepsilon_{Si} \quad (12a)$$

$$B_{ds} = A_{ss} e^{(\phi_{ds}-\phi_{FD})/v_{th}} - \left[C_{ox}\left(V_{gf} - (\phi_{ds} - \phi_{FD})\right) \big/ \varepsilon_{Si} \right]^2 \quad (12b)$$

in which $X_o = \min(X_{dm}, X_{d,FD})$. This model gives better doping dependence of ϕ_o in strong inversion without assuming a constant difference from ϕ_s, as shown in Fig. 3(b), which is only possible with the URM approach. The unified regional ϕ_o solution in accumulation can be similarly obtained [2].

2.2 Body-Thickness Scaling

In bulk or PD-SOI devices, body doping is usually very high, and short-channel effects (SCEs) due to 2D transverse field near the S/D are limited by the maximum depletion width that is usually in the submicron range. For UTB-SOI and DG/GAA devices, the body is usually undoped or unintentionally doped and it is very thin such that 2D transverse-field effect is very small. However, just as in bulk-model formulations, which start from ideal long-channel equations and adding SCEs for short-channel devices, model formulations for DG/GAA devices should also approach correct physical behaviors in thick-body even if they do not practically exist. A model that can only be applied to thin-body (which is "long-channel" like) devices may have incorrect reference potential when it is extended to thick-body ("short-channel" like) devices.

Body-thickness dependence should be reflected in the quasi-2D Poisson's solution for the surface-potential "lowering" from the long-channel ϕ_s:

$$\delta\phi_{s,c}(y) = \left(V_{bi,c} + V_c - \phi_s\right) \frac{\sinh\left[(L-y)/\lambda\right]}{\sinh(L/\lambda)} \quad (c = s, d) \quad (13)$$

where $\lambda = \varepsilon_{Si} X_o / \eta C_{ox}$ and $X_o = \min\{X_{dm}, T_{Si}/2 \text{ (s-DG)}\}$, and $V_{bi,s/d}$ is the S/D–body pn-junction built-in potential. The drain-induced barrier lowering (DIBL) model, which also includes T_{Si}-dependent flatband voltage, is included in V_{FB}, in which $\delta\phi_s$ is based on (13) at $y = L/2$ [2]:

$$\delta\phi_s \equiv \delta\phi_{s,s}(L/2) + \delta\phi_{s,d}(L/2) = \left(V_{bi,s} + V_{bi,d} + \alpha_{dibl}(V_s + V_d) - 2\phi_s\right) \frac{1}{2\cosh(L/2\lambda)} \quad (14)$$

where η and α_{dibl} are fitting parameters.

Figures 4 shows the surface potential versus gate voltage for the $L = 100$-µm device. Near-unity slope is observed in (b) for $T_{Si} < 20$ µm, indicating transition into volume-inversion behavior. For $T_{Si} > 30$ µm, a V_g-dependent slope in the subthreshold can be observed, which is due to the tails of the 2D potentials merging. Figure 4(c) further illustrates these behaviors for the $L = 10$-µm device: when $T_{Si} > 5$ µm, severe thick-body effects (TBEs, or SCEs) occur, as modeled by the quasi-2D ϕ_s model (14).

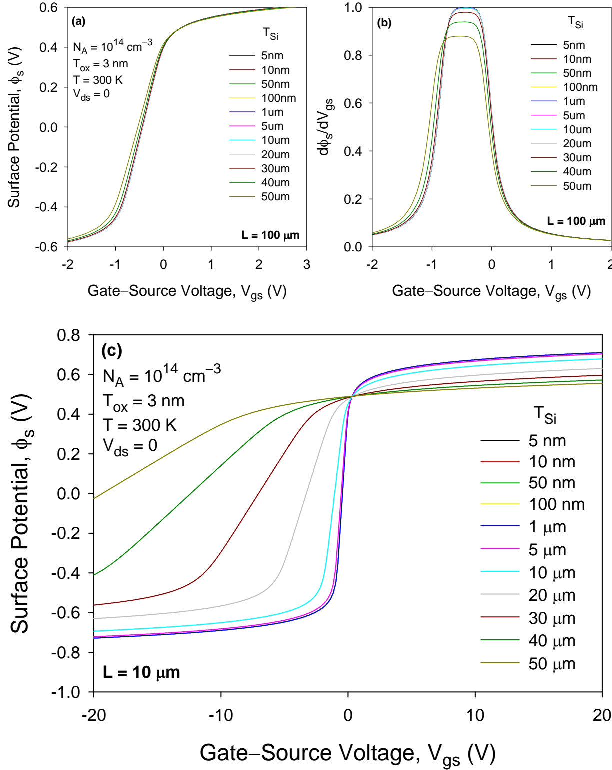

Figure 4: (*a*) Surface potential of the $L = 100$-µm device at various body thickness as indicated and (*b*) its derivative w.r.t. V_{gs}, showing SCEs due to S/D pn-junction depletions when $T_{Si} > 30$ µm. (*c*) For the $L = 10$-µm device, SCEs are observable when $T_{Si} > 5$ µm [6].

2.3 Body Contact

For body-contacted (BC) MOSFETs, the reference potential (hole imref for nMOS) is set to the body bias, $V_r = V_b$. The ZF potential in bulk and PD-SOI will be set to $\phi_o = V_b = 0$. As long as the drain-current model is a strictly odd function of V_{ds} and no singularities at $V_{ds} = 0$, Gummel symmetry test (GST) can be satisfied. For MOSFETs without BC, such as FB-SOI and DG/GAA devices, GST can be similar if only FD (volume inversion) occurs. However, for FB PD-SOI, since the reference potential $V_r = \min\{V_s, V_d\}$, there will be a region where $\phi_o = V_r$ gives "abrupt changes" around $V_{ds} = 0$, due to the ϕ_{dd} term in (8) that gives a glitch in higher-order GST. Physically, this is due to the unipolar assumption (hole imref being a constant), which shows its effect only at extremely low current levels when the electron current is comparable to the (missing) hole current. Such a behavior (in higher-order GST) can also be seen in *unipolar* numerical device simulations.

This problem can be solved by the "symmetric imref correction" (SIC) for physically modeling ϕ_o based on balancing the two back-to-back S/D pn-junction diode currents, given by [2]

$$\phi_o = nv_{th}\left[\ln 2 - \ln\left(e^{-V_s/nv_{th}} + e^{-V_d/nv_{th}}\right)\right] \quad (15)$$

where n is taken as a fitting parameter. Results of 3rd-order harmonic-balance test (HBT) confirm the SIC model, as shown in Fig. 5.

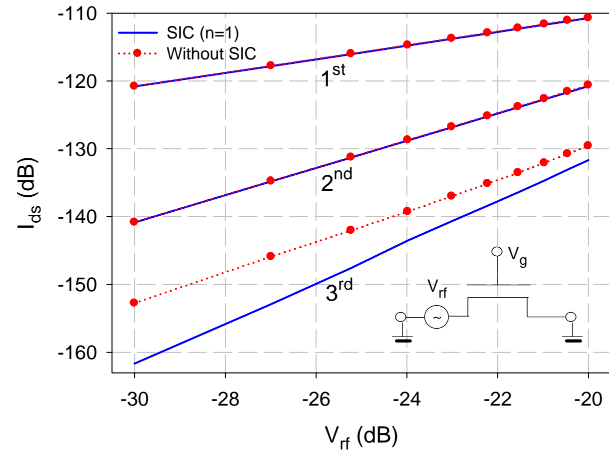

Figure 5: HBT to the 3rd order, with or without the SIC [3].

The same idea has been extended to model the "kink effect" in FB-SOI, in which ϕ_o is modeled by [2]

$$\phi_o = nv_{th}\left[\ln\left(2 + \frac{I_{ii}}{I_s}\right) - \ln\left(e^{-V_s/nv_{th}} + e^{-V_d/nv_{th}}\right)\right] \quad (16)$$

where I_{ii} is the impact-ionization current and I_s is the S/D diode reverse saturation current. This leads to an *explicit* model for the FB effect without the need to introduce an internal circuit node.

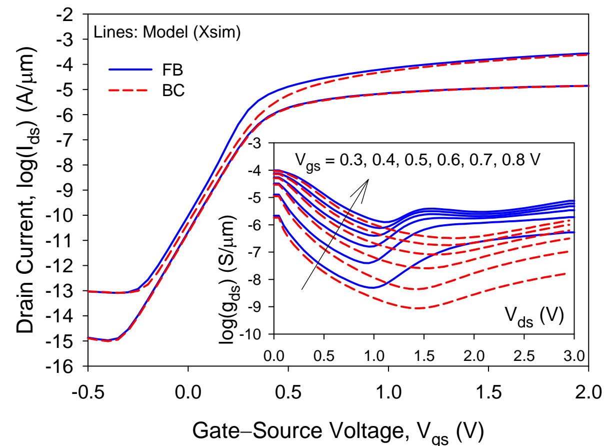

(a)

NSTI-Nanotech 2011, www.nsti.org, ISBN 978-1-4398-7139-3 Vol. 2, 2011

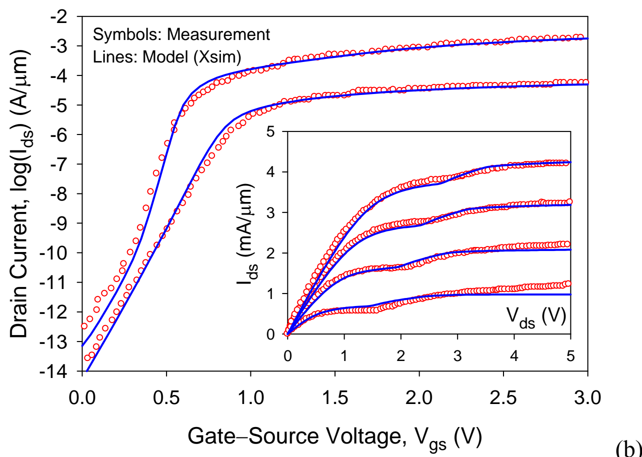

Figure 6: (*a*) Modeled transfer I_{ds} vs. V_{gs} and output conductance g_{ds} vs. V_{ds} (inset) characteristics for FB-SOI (*solid*) and BC-SOI (*dashed*). (*b*) Modeled (*lines*) linear and saturation log(I_{ds}) vs. V_{gs}, compared with the measured device (*symbols*). The inset shows the same for the I_{ds} vs. V_{ds} characteristics.

2.4 Source/Drain Contact

As long as heavily-doped pn-junction S/D is used, unipolar transport can be assumed since essentially no source and sink for holes in such an nMOSFET, except for the missing hole current in higher-order GST/HBT that has been remedied by the SIC, and the small (nV) error in ϕ_s of the PB solution due to ignoring holes as benchmarked from the rigorous two-carrier solution [7]. However, for Schottky-barrier (SB) [8] or dopant-segregated Schottky (DSS) [9] MOSFETs, ambipolar transport has to be modeled, together with quasi-2D potential solutions and tunneling current calculations.

The Xsim model based on defining "source" and "drain" by the device labels ("S/D by label" i.e., by layout), rather than by convention, allows separate source and drain current formulations. Source/drain contacts can be modeled independently and symmetrically, and extendable to modeling asymmetric S/D [10].

3 SUMMARY AND CONCLUSIONS

The unique URM approach provides correct asymptotic physical solutions and approximate ones in seamless transitions across different regions of operation for various types of MOSFETs. It gives a consistent framework for building multilevel models within the same core structure: the s-DG FinFET (also GAA SiNW) is similar to the bulk formulation, the ca-DG FinFET and PD/FD-SOI are two variations, while the ia-DG FinFET is the most general device that includes all other types as special cases. Unification of MOS models in one single core not only reduces duplicating efforts, but also provides an infrastructure for modeling hybrid technologies with different types of devices on the same chip, as well as selectable accuracy for design simulations and verifications using the same parameter set.

Acknowledgement: The group as well as the Xsim model development has been supported by Semiconductor Research Corp. (SRC), Globalfoundries (GF) Singapore, Institute of Microelectronics (IME), Institute for Sustainable Nanoelectronics (ISNE), and Nanyang Technological University (NTU).

REFERENCES

[1] J. Watts, C. McAndrew, C. Enz, C. Galup-Montoro, G. Gildenblat, C. Hu, R. van Langevelde, M. Miura-Mattausch, R. Rios, and C-T Sah, "Advanced compact models for MOSFETs," in *Proc. WCM-Nanotech 2005*, Anaheim, CA, May 2005, vol. WCM, pp. 3–12.

[2] X. Zhou, G. J. Zhu, G. H. See, K. Chandrasekaran, S. B. Chiah, and K. Y. Lim "Unification of MOS compact models with the unified regional modeling approach," (*Invited*), *J. Comput. Electron.*, Mar. 2011 [http://www.springerlink.com/content/x8t0742r3m051650/].

[3] X. Zhou, G. J. Zhu, M. K. Srikanth, S. H. Lin, Z. H. Chen, J. B. Zhang C. Q, Wei, Y. F. Yan, R. Selvakumar, and Z. H. Wang, "Xsim: Benchmark tests for the unified DG/GAA MOSFET compact model," in *Proc. NSTI Nanotech 2010*, Anaheim, CA, Jun. 2010, vol. 2, pp. 785–788.

[4] R. H. Kingston and S. F. Neustadter, "Calculation of the space charge, electric field, and free carrier concentration at the surface of a semiconductor," *J. Appl. Phys.*, vol. 26, no. 6, pp. 718–720, Jun. 1955.

[5] W. Z. Shangguan, X. Zhou, K. Chandrasekaran, Z. M. Zhu, S. C. Rustagi, S. B. Chiah, and G. H. See, "Surface-potential solution for generic undoped MOSFETs with two gates," *IEEE Trans. Electron Devices*, vol. 54, no. 1, pp. 169–172, Jan. 2007.

[6] X. Zhou, G. J. Zhu, M. K. Srikanth, S. H. Lin, Z. H. Chen, J. B. Zhang, and C. Q. Wei, "A unified compact model for emerging DG FinFETs and GAA nanowire MOSFETs including long/short-channel and thin/thick-body effects," (*Invited Paper*), in *Proc. ICSICT2010*, Shanghai, China, Nov. 2010, pp. 1725–1728.

[7] X. Zhou, Z. M. Zhu, S. C. Rustagi, G. H. See, G. J. Zhu, S. H. Lin, C. Q. Wei, and G. H. Lim, "Rigorous surface-potential solution for undoped symmetric double-gate MOSFETs considering both electrons and holes at quasi nonequilibrium," *IEEE Trans. Electron Devices*, vol. 55, no. 2, pp. 624–631, Feb. 2008.

[8] G. J. Zhu, X. Zhou, T. S. Lee, L. K. Ang, G. H. See, S. H. Lin, Y. K. Chin, and K. L. Pey, "A compact model for undoped silicon-nanowire MOSFETs with Schottky-barrier source/drain," *IEEE Trans. Electron Devices*, vol. 56, no. 5, pp. 1100–1109, May 2009.

[9] G. J. Zhu, X. Zhou, Y. K. Chin, K. L. Pey, J. B. Zhang, G. H. See, S. H. Lin, Y. F. Yan, and Z. H. Chen, "Subcircuit compact model for dopant-segregated Schottky gate-all-around Si-nanowire MOSFETs," *IEEE Trans. Electron Devices*, vol. 57, no. 4, pp. 772–781, Apr. 2010.

[10] G. H. See, X. Zhou, K. Chandrasekaran, S. B. Chiah, Z. M. Zhu, C. Q. Wei, S. H. Lin, G. J. Zhu, and G. H. Lim, "A compact model satisfying Gummel symmetry in higher order derivatives and applicable to asymmetric MOSFETs," *IEEE Trans. Electron Devices*, vol. 55, no. 2, pp. 616–623, Feb. 2008.